Separation Science and Technology
Publication details, including instructions for authors and subscription information:
http://www.informaworld.com/smpp/title~content=t713708471

Separation Mechanisms in Gel Permeation Chromatography

W. W. Yau[a]; C. P. Malone[a]; H. L. Suchan[a]
[a] ENGINEERING PHYSICS LABORATORY, E. I. DU PONT DE NEMOURS & CO., INC., WILMINGTON, DELAWARE

To cite this Article Yau, W. W. , Malone, C. P. and Suchan, H. L.(1970) 'Separation Mechanisms in Gel Permeation Chromatography', Separation Science and Technology, 5: 3, 259 — 271
To link to this Article: DOI: 10.1080/01496397008080031
URL: http://dx.doi.org/10.1080/01496397008080031

SEPARATION SCIENCE, 5(3), pp. 259–271, June, 1970

Separation Mechanisms in Gel Permeation Chromatography

W. W. YAU, C. P. MALONE, and H. L. SUCHAN

ENGINEERING PHYSICS LABORATORY,
E. I. DU PONT DE NEMOURS & CO., INC.
WILMINGTON, DELAWARE 19898

Summary

This paper presents flow rate studies, vacancy chromatography, and a static mixing experiment. Data obtained on an unpacked column (a straight tube) and on a column packed with nonporous glass beads are also reported. The results reveal that peak dispersion in GPC arises mainly from lateral diffusion in the stationary phase (permeation in and out of the porous substrate) and from lateral diffusion in the mobile phase. GPC peak separation is mainly dominated by the process of steric exclusion. Pore size distribution data obtained on Bio-Rad porous glass are shown to illustrate the preference of random coil theories over theories of the equivalent sphere in the interpretation of steric exclusion of flexible polymers. The data are discussed in terms of Herman's diffusion theory and Cassasa's exclusion theory.

INTRODUCTION

Since the development of gel permeation chromatography (GPC) as a means to determine molecular weight distribution of flexible polymers, considerable interest has been shown in studying the separation mechanism. An understanding of the basic mechanism of GPC has great importance as a guide for such studies of practical interest as the improvement of separation efficiency, the correction for peak dispersion (*1*), and the development of a universal calibration curve (*1*).

Models have been proposed to explain GPC in terms of separation by flow (*2*), separation by restricted diffusion (*1*), and separation by steric exclusion (*1*). Since all of these postulated processes may occur in a GPC experiment, interpretation based on one model alone is not

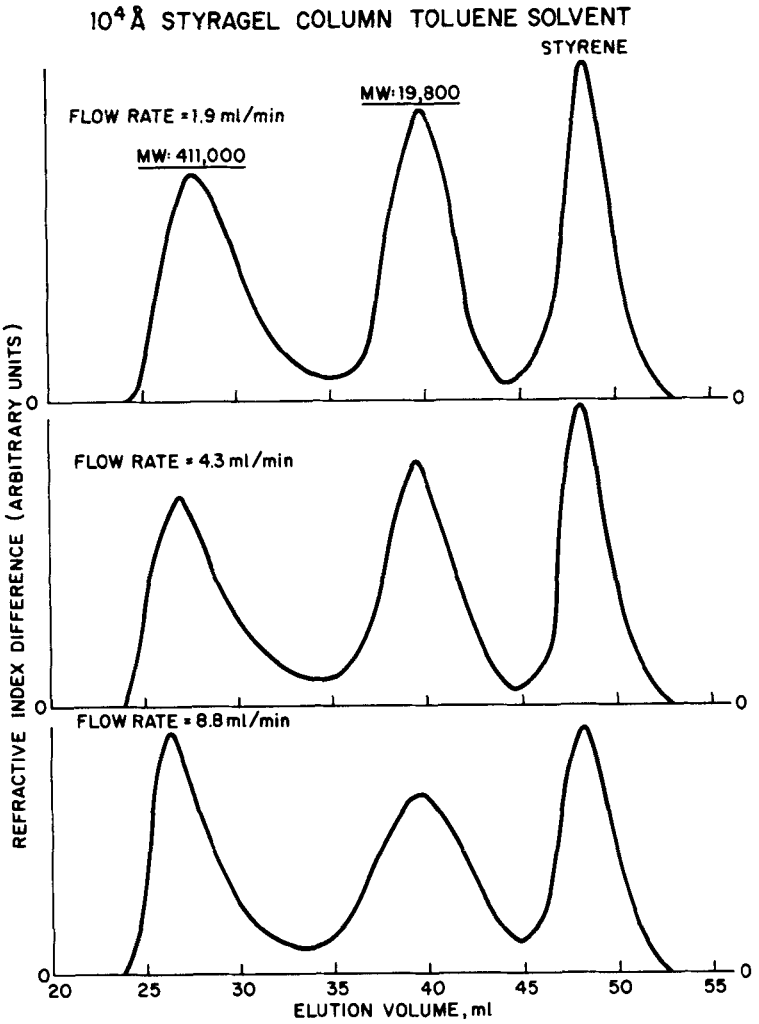

FIG. 1. Effect of flow rate on GPC curve shape.

sufficient to explain fully both the dispersion and the separation of GPC peaks. In the following, some experimental results are presented to show the relative importance of each of the postulated processes to GPC peak dispersion and GPC peak separation.

GPC data reported in this work were obtained either on a Waters Associates apparatus with a differential refractometer or on a GPC unit with the Du Pont Model 400 photometric analyzer as an ultra-

violet detector. The polystyrene standards of narrow molecular weight distribution ($\bar{M}_w/\bar{M}_n < 1.10$) used in the experiments were obtained from Pressure Chemical Company, except for MW 4800, which was obtained from Waters Associates.

PEAK DISPERSION

The GPC elution curves obtained at three flow rates for a composite solution of styrene and two polystyrene standards are shown in Fig. 1. Peak dispersion changes with molecular size and with flow rate. As illustrated in Fig. 1, peak dispersion in GPC is greater at higher flow rates and for species of higher molecular weight except for those eluted near the void volume. The dispersion of peaks near the void volume, such as the peak of MW 411,000, will be discussed later. These observations imply that it is not longitudinal diffusion (in the flow direction) but lateral diffusion that is responsible for the dispersion of GPC peaks. In the case of longitudinal diffusion, the dispersion would be smaller for species of higher molecular weight (smaller diffusion coefficient) and would decrease with increasing flow rate (decreasing retention time). On the other hand, the results can be very well understood in terms of lateral diffusion processes, such as extra-column dispersion, permeation, and lateral diffusion in the mobile phase, which are described in the following paragraphs.

The characteristics of the extra-column dispersion are illustrated in Fig. 2, which shows the elution peak of styrene and that of polystyrene of MW 1.8×10^6 after passing through a tubing of small diameter. The dispersion of these peaks can be explained as the result of the velocity profile in the flow stream. The difference between the two curves is caused by the difference in the lateral diffusion rate between the two systems. As a solute band travels through the tubing, it becomes increasingly distorted due to the velocity profile. The center portion of the band travels faster, but it is less distorted than the outer portion near the wall of the tubing. In case of negligible lateral diffusion such a distorted band is expected to give an elution peak with a sharp front and a long tail, such as that observed for the polystyrene peak shown in Fig. 2. The distortion of the solute band also creates concentration gradients in the radial direction of the tubing. This concentration gradient is negative at the leading edge of the band; therefore, the solute molecules tend to diffuse from the center of the tubing to the slow-moving region near the wall. The reverse is true at the tailing edge of the band. This implies that a fast rate of lateral dif-

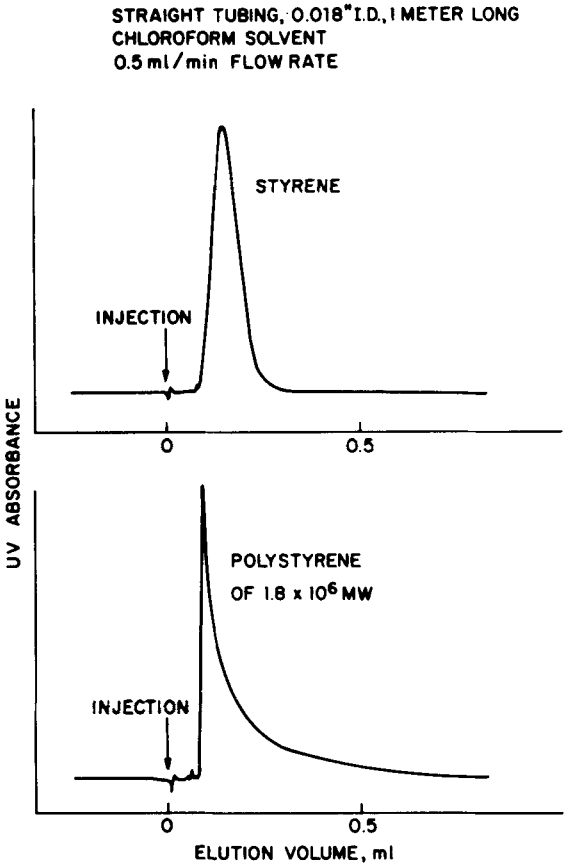

FIG. 2. Extra-column dispersion in GPC.

fusion tends to give a symmetrical elution peak, and this seems to be the case for the styrene peak shown in Fig. 2.

By comparing Figs. 1 and 2, it is obvious that GPC peak dispersion is not explained by the capillary model (*2*) proposed to describe GPC separation. The dispersion predicted by such a model, as one may visualize by extrapolating the results in Fig. 2 to large retention volume, would be orders of magnitude larger than what is observed in Fig. 1. This suggests that the packing in a GPC column must have sufficiently distorted the flow stream to prevent the development of a persistent velocity profile in the column.

To prove the above hypothesis, GPC elution curves of the styrene

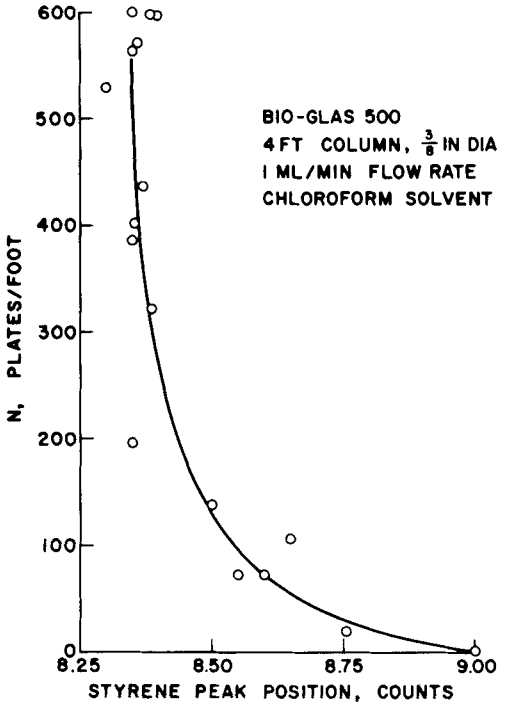

FIG. 3. Effect of packing density on GPC peak dispersion.

solution were obtained on a column which was repeatedly packed with different amounts of Bio-Glas 500 glass beads. At each packing density, the number of theoretical plates per unit column length (*3*), N, was calculated according to the approximate formula, $N \cong 4Ve^2/LW^2$, where Ve is the peak elution volume, L is the column length, and W is the peak half-width. Figure 3 shows how N decreases with increasing peak elution volume, i.e., with decreasing packing density. This is what one would expect from the disrupture of a persistent velocity profile mentioned in the previous paragraph.

Flow rate data obtained on columns packed with smooth, nonporous glass beads were used by Kelley and Billmeyer (*4*) to explain the mechanism of mobile phase dispersion in GPC. These authors showed that the experimental results were in good agreement with a coupling theory they developed [similar to that of Giddings' theory (*3*)], in which they interpreted the lateral diffusion as being caused by the velocity nonuniformity across the column cross section. The results

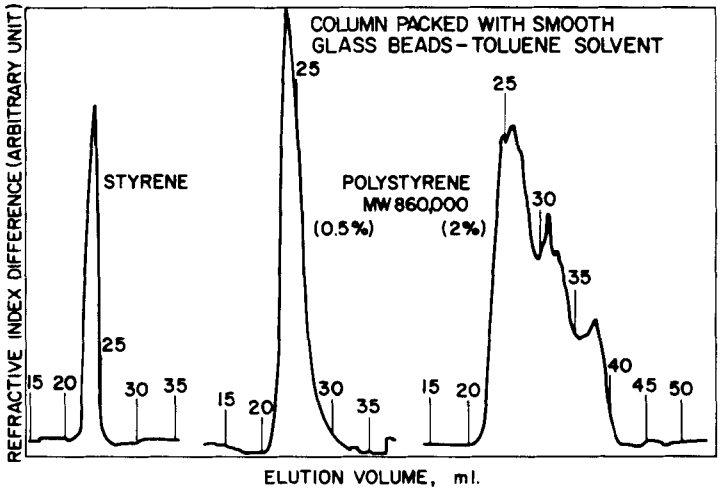

FIG. 4. Mobile phase dispersion in GPC.

of this study confirm that mobile phase dispersion plays an important role in GPC. It contributes a great deal to GPC dispersion because of the low diffusion coefficients of the polymer molecules.

The magnitude of mobile phase dispersion is illustrated in Fig. 4, which shows the elution curves of styrene and the polystyrene samples of MW 860,000 obtained on a column packed with smooth glass beads. The curve obtained for the polystyrene sample at 2% solution concentration is included in Fig. 4 to demonstrate that the so-called "overloading effect" can also happen in a column of nonporous packing. This would suggest that, whatever the causes of such an effect may be, it should not be considered in terms of oversaturation of the porous volume as the word "overloading" would imply. Comparing Figs. 1 and 4, one sees that the width of curves shown in Fig. 4 are of comparable magnitude to, yet are appreciably smaller than, those shown in Fig. 1. This indicates that permeation as well as mobile phase dispersion should be considered to fully account for GPC peak dispersion.

Both the extent and the rate of permeation are the important factors dictating the amount of dispersion caused by permeation. For this reason the stochastic model (*5*), which is derived on the basis of the extent of permeation only, is inadequate to describe GPC dispersion. The prediction of this model, viz., that dispersion increases with increasing retention volume, is not substantiated by the GPC results. A complete description of permeation dispersion was recently

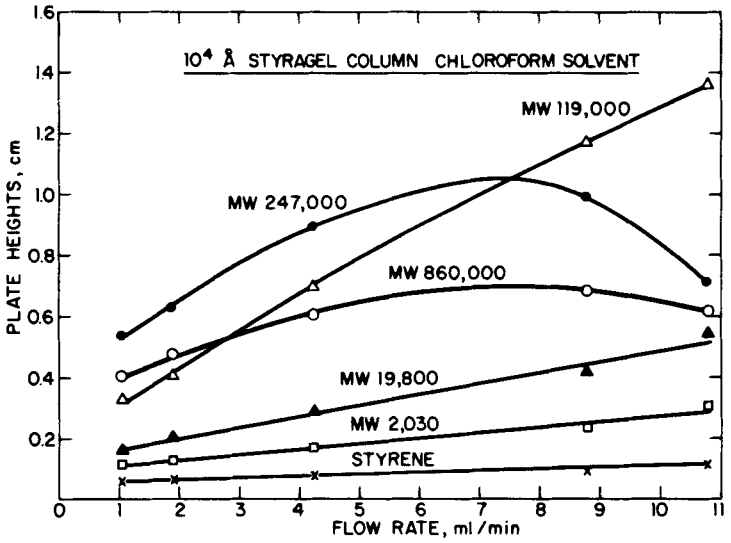

FIG. 5. Effect of flow rate on GPC peak dispersion.

developed by Hermans (*6*). In the following paragraphs the principal implications of his theory are briefly described and are compared with the results of the flow rate study on a 10^4 Å Styragel column which is shown in Fig. 5. This figure shows the dependence of the peak dispersion of several polystyrene samples of different molecular weight (MW) and the styrene solution, in which the plate height (*3*) of the elution peak, approximated by the quantity $LW^2/4Ve^2$, is plotted versus flow rate, where the symbols L, W, and Ve are the same as defined previously.

In the case of fast permeation, Herman's theory predicts [Eq. (38) in Ref. *6*] that the mean square fluctuation in retention volume should be proportional to u/kD_s. (Where u, k, and D_s are the symbols used by Hermans to represent the average flow velocity, the ratio of the concentration in the mobile phase versus that in the stationary phase, and the solute diffusion coefficient in the stationary phase, respectively. One may notice that the ratio k is a parameter to express the extent of permeation. It is equal to $1/K$, where K is the often-used symbol of the distribution coefficient.) Physically, this means the following: (*a*) at a fast diffusion rate, the peak dispersion, or plate height, should increase linearly with increasing flow rate (which is indeed observed for the curves of styrene and polystyrene of MW, 2,030, 19,800, and

119,000 shown in Fig. 5); (*b*) the dependence of peak dispersion on MW should be governed by the linear relationship between W^2 and $1/kD_s$. Since D_s decreases, yet k increases, with increasing MW, one should expect peak dispersion caused by permeation to increase with increasing MW until the product kD_s reaches a minimum, then to decrease with further increasing MW as k becomes increasingly large. In the extreme case, when no permeation occurs, k is infinitely large, the contribution of permeation dispersion is zero and the peak width should be affected only by the mobile phase dispersion. [This may explain the lower dispersion level of the peak of 860,000, relative to that of MW 247,000 and 119,000, shown in Fig. 5. The molecules of MW 860,000, which are eluted at the void volume of the column, are totally excluded from the Styragel packing in the column. The peak is less dispersed since it does not have, in contrast to the other ones, the contribution from permeation dispersion. The fact that the curve of MW 860,000 is relatively flow rate-independent is in agreement with the above reasoning, since it has been reported (*4*) that, for highly dispersed peaks, the mobile phase dispersion becomes flow rate-independent as a consequence of the coupling effect.]

For insufficient permeation rates, Hermans' theory predicts a highly dispersed and skewed elution peak. Insufficient permeation rate is defined here as the experimental condition under which the solution molecules do not have sufficient time to establish equilibrium between the mobile and the stationary phases. Such a condition is more likely to be true at high flow rates and for large solute molecules. From the concentration profile of such an elution peak [given in Eq. (26) in Ref. *6*], can show that, under nonequilibrium condition, W^2 should vary linearly with D_s^2/k^4u^2, i.e., W should decrease with increasing flow rate. (This seems to be the reason for the decline of the curve of MW 247,000 in the high flow rate region shown in Fig. 5.) These results indicate that nonequilibrium is not realized under the normal operating condition of GPC. It becomes noticeable only at very high flow rate and for samples of high MW.

PEAK SEPARATION

Diffusion models (*1*) have been proposed that assume peak separation in GPC is caused by the nonequilibrium mechanism mentioned in the previous paragraph. In view of the results discussed above, it is obvious that such a model would not be adequate to account for the overall peak separation in GPC. The rate of permeation would

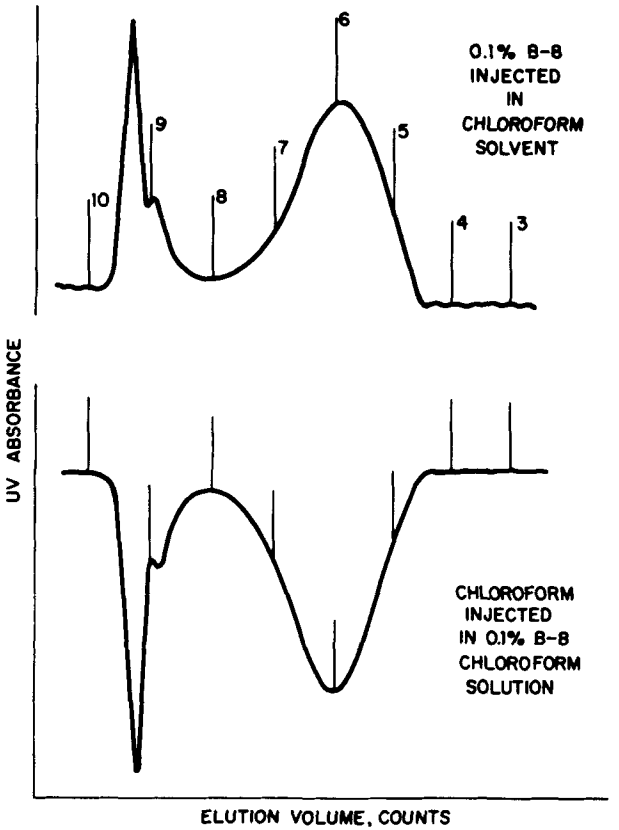

FIG. 6. Conventional and vacancy GPC elution curves.

affect peak separation only at high flow rate and for samples of high MW. This is reflected in the fact that GPC peak positions, except the ones of high MW, are virtually flow rate-independent.

A capillary model (*2*) has recently been proposed to explain GPC peak separation. The model assumes that GPC separation is the result of the capillary velocity profile in combination with a wall effect that causes the larger solute molecules being more populated near the center of the flow stream, therefore having a larger average flow velocity. Experimental evidence against such a model is provided in the results shown in Figs. 4 and 6. The fact that the styrene and the polystyrene peaks both elute near the void volume of a column packed with smooth glass beads (see Fig. 4) shows that the velocity profile in the interstitial spaces does not provide the separation capability.

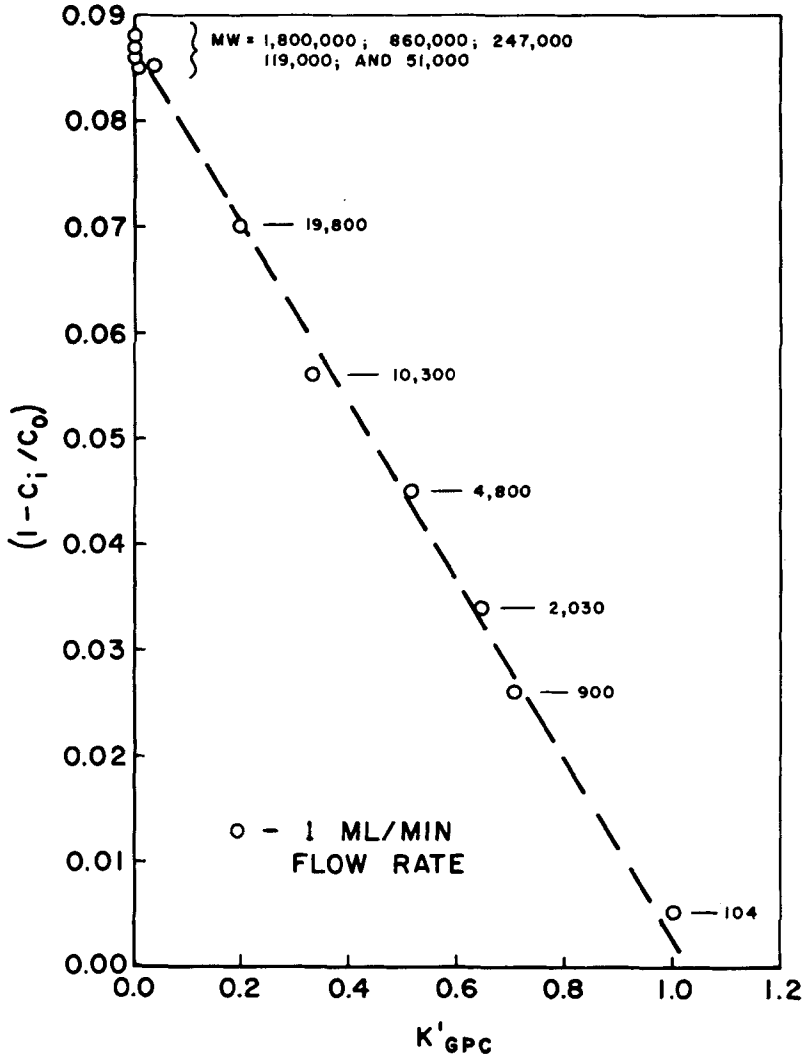

FIG. 7. Comparison of polymer-gel mixing data with GPC data.

The fact that the vacancy elution curve (7), obtained by an injection of solvent into the flow stream of the polymer solution, is characteristic of the polymer and not of the solvent (see Fig. 6), is also in direct contradiction to the capillary model. The conventional (top curve) and the vacancy (bottom curve) GPC elution curves shown in Fig.

6 were obtained on a 10^4 Å Styragel column for a polystyrene standard, designated B-8, obtained from Dow Chemical Company. These results indicate that the porous nature of the GPC packing, which is neglected in the capillary model, is the essential element of the separation capability in GPC.

The results discussed so far have indicated that kinetic processes contribute only in minor ways to the peak separation in GPC. This suggests that an equilibrium mechanism, viz., the extent of permeation, must be the origin of GPC peak separation. Direct experimental evidence for this contention is provided by a static experiment of polymer–gel mixing (*8*). The result of such an experiment is illustrated by Fig. 7 with data obtained on Bio-Glas 200 Å glass beads. Figure 7 shows that there is a change from an initial concentration C_i to a final concentration C_0 when a polymer solution is mixed with dry porous material. This concentration change is a function of MW of the polystyrene samples; therefore, it too depends on the distribution coefficient K'_{GPC}. K'_{GPC} is defined as $(V_e - V_0)/(V'_t - V_0)$, where V_e and V'_t are the GPC elution volumes of the polystyrene and the styrene peaks, respectively, and V_0 is the void volume of the GPC column. The linear relationship between $(1 - C_i/C_0)$ and K'_{GPC} shown in Fig. 7 indicates that the separation achieved in this GPC column is due to a distribution of the solute molecules between the mobile and the stationary phases which closely approximates the equilibrium condition.

These results demonstrate that GPC separates primarily by the extent to which the solute molecules can permeate the porous packing. Several theories based on steric exclusion have been proposed to explain the effect of the size of a flexible polymer molecule on the extent of permeation. The earlier models (*1*) assume that the exclusion effect of a flexible polymer molecule can be approximated by that of a rigid sphere with a radius equivalent to the radius of gyration of the molecule. As de Vries et al. (*4*) have pointed out, such a model is not adequate to explain GPC peak separation of flexible polymer molecules since the shape of the GPC calibration curve for flexible polymer molecules is different from the pore size distribution curve of the packing. Such a comparison is given in Fig. 8. The dashed curve is the pore size distribution curve of Bio-Glas 500 Å porous glass, and the data points identified by △ are the GPC results obtained on a column packed with the same glass.

Models of steric exclusion based on thermodynamic reasonings have recently been proposed. The theory for rigid molecules was developed

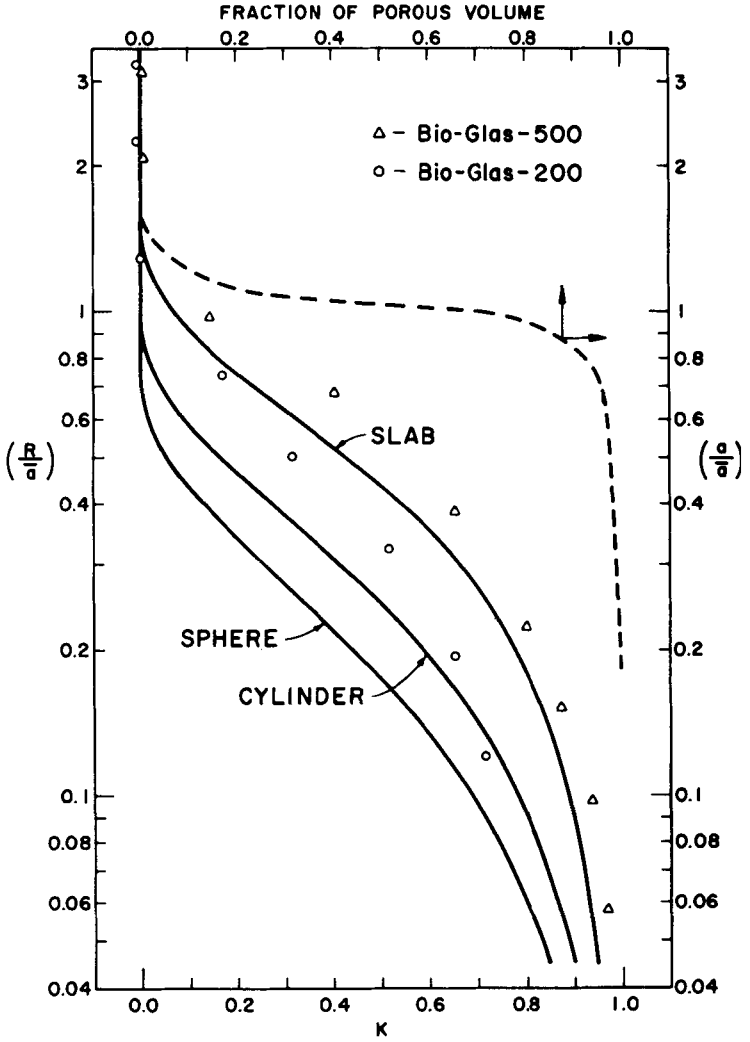

FIG. 8. Comparison of GPC data with pore size distribution curve and with Casassa's theoretical curves.

by Giddings et al. (*10*). The theory for flexible polymer molecules was developed by Casassa (*11*). An approximate treatment of the problem was given in the stochastic model (*5*). Cassassa explained the decrease in the extent of permeation with increasing MW of the flexible polymer molecules as a consequence of the decrease in the conformational

freedom of such a molecule in the pores of the GPC packing. For a pore of either sphere, cylinder, or slab shape, he derived the theoretical expression for the distribution coefficient (K) of the solute molecule as a function of the radius of gyration of the molecule (R) and the size of the pore ($\bar{a}$) [Eqs. (2), (3) and (4) in Ref. *11*]. The solid lines in Fig. 8 show the theoretical curves predicted by the theory (from top to bottom: slab, cylinder, sphere). They compare well with the GPC results obtained on a column packed with Bio-Glas 500 Å (plotted by △) and with Bio-Glas 200 Å (plotted by ○). Obviously, Casassa's theory describes the shape of the GPC calibration curve much better than the earlier equivalent sphere models. This implies that the curvature of the GPC calibration curve is very much determined by the fluctuating nature of the polymer molecule. Therefore, the extent to which the calibration curve can be flattened to give better peak separation by improving the sharpness of the pore size distribution of the packing is limited.

Pore size distribution measurements were provided by the American Instrument Company. The average pore radius ($\bar{a}$) is 63.2 Å for Bio-Glas 200 Å as determined by nitrogen desorption, and 210 Å for Bio-Glas 500 Å as determined by mercury intrusion.

REFERENCES

1. K. H. Altgelt, in *Advances in Chromatography,* Vol. 7 (J. C. Giddings and R. A. Keller, eds.), Dekker, New York, 1968, pp. 3–46.
2. E. A. Di Marzio and C. M. Guttman, *J. Polym. Sci., Part B,* **7,** 267 (1969).
3. J. C. Giddings, *Dynamics of Chromatography. Part 1. Principles and Theory,* Dekker, New York, 1965.
4. R. N. Kelley and F. W. Billmeyer, Jr., *Anal. Chem.,* **41,** 874 (1969).
5. J. B. Carmichael, *J. Polym. Sci., Part A-2,* **6,** 517 (1968).
6. J. J. Hermans, *J. Polym. Sci., Part A-2,* **6,** 1217 (1968).
7. C. P. Malone, H. L. Suchan, and W. W. Yau, *J. Polym. Sci., Part B,* **7,** 781 (1969).
8. W. W. Yau, C. P. Malone, and S. W. Fleming, *J. Polym. Sci., Part B,* **6,** 803 (1968).
9. A. J. de Vries, M. Le Page, R. Beau, and C. L. Guillemin, *Anal. Chem.,* **39,** 935 (1968).
10. J. C. Giddings, E. Kucera, C. P. Russell, and M. N. Myers, *J. Phys. Chem.,* **72,** 4397 (1968).
11. E. F. Casassa, *J. Polym. Sci., Part B,* **5,** 773 (1967).

Received by editor October 3, 1969